ISSN 0030-400X, Optics and Spectroscopy, 2012, Vol. 113, No. 5, pp. 517–521. © Pleiades Publishing, Ltd., 2012.
Original Russian Text © S.Ya. Vetrov, A.Yu. Avdeeva, R.G. Bikbaev, I.V. Timofeev, 2012, published in Optika i Spektroskopiya, 2012, Vol. 113, No. 5, pp. 571–575.

NONLINEAR AND QUANTUM OPTICS

Traveling of Light through a 1D Photonic Crystal Containing a Defect Layer with Resonant Dispersion

S. Ya. Vetrov[a, b], A. Yu. Avdeeva[a], R. G. Bikbaev[a], and I. V. Timofeev[a, b]

[a] *Siberian Federal University, Krasnoyarsk, 660074 Russia*

[b] *Kirensky Institute of Physics, Siberian Branch, Russian Academy of Sciences, Krasnoyarsk, 660036 Russia*

e-mail: s.vetrov@inbox.ru, avdeeva-anastasiya@yandex.ru

Received March 12, 2012

Abstract—Spectral properties of a 1D photonic crystal that is comprised of two multilayered dielectric mirrors and a nanocomposite layer between them as a structural defect are studied. The nanocomposite consists of silver nanoballs dispersed in a transparent matrix and is characterized by an effective resonant permittivity. The spectral manifestation of the defect mode splitting for the *s*-polarized waves is studied as a function of the angle of incidence and concentration of nanoballs. Specific features of the transmission spectra for the *s*- and *p*-polarized waves are established for the angle of incidence equal to the Brewster angle of the seeding photonic crystal. It is shown, in particular, that, in the region of the continuous transmission spectrum of the *s*-polarized waves, there arises an additional bandgap caused by mixing of the resonant mode with photonic modes.

DOI: 10.1134/S0030400X12110070

INTRODUCTION

A fundamental property of photonic crystals (PhCs) is related to the localization of electromagnetic waves on defects of the structure. In this case, additional allowed levels that correspond to localized modes arise in bandgaps of PhCs. The position and transmission coefficient of defect modes can be efficiently controlled by varying geometrical and structural parameters of the PhC. New types of photonic-crystal waveguides [1], high-Q nanocavities [2, 3], and low-threshold lasers [4] have been created based on PhCs with defect modes, and ways to enhance nonlinear optical processes have been proposed [5–7].

Composite media with metal nanoparticles intended for creating nanostructured metal-dielectric photonic crystals and new methods of light control based on them are of interest [8, 9]. A nanocomposite comprised of metal nanoparticles suspended in a transparent matrix is characterized by a resonant effective permittivity [10, 11], whereas the optical characteristics of initial materials do not show any resonant features. The position of the resonance lying in the visible range depends on the permittivity of initial materials, as well as on the concentration and shape of nanoparticles. For the case of ρ-polarized waves, specific features have been studied in [12] of spectral properties of a one-dimensional photonic crystal with the resonant defect layer of a nanocomposite comprised of spherical silver nanoparticles randomly distributed over a dielectric matrix.

In this paper, as distinct from [12], we studied the transmission spectrum for *s*-polarized waves in the framework of a 1D PhC with a resonant defect layer of a nanocomposite. We studied possibilities of controlling the defect mode splitting of such a PhC by varying the volume fraction of nanoballs in the defect layer and the angle of incidence. Specific features of the transmission spectrum for *s*- and *p*-polarized waves at an angle of incidence equal to the Brewster angle of the seeding PhC were examined.

STARTING MODEL

The PhC under study is a finite stratified medium consisting of alternating layers of two materials with a structural lattice defect. As a defect layer, we chose a nanocomposite layer W_d thick comprised of metal nanoballs dispersed in a transparent matrix. The defect layer is sandwiched between two identical superlattices with an elementary cell consisted of layers of materials a and b with thicknesses W_a and W_b, respectively. The nanocomposite layer is characterized by effective permittivity of the nanocomposite $\varepsilon_{mix}(\omega)$. In what follows, we assume that the structure under consideration is bounded by vacuum from the left and from the right and the plane monochromatic light wave is incident upon the PhC structure at angle θ. Permittivity ε_{mix} is determined by the Maxwell–Garnett formula, which is commonly used to describe matrix media, when separate inclusions of small volume fraction are dispersed in the matrix material [11, 13]:

$$\varepsilon_{mix} = \varepsilon_d \left[1 + \frac{f}{(1-f)/3 + \varepsilon_d/(\varepsilon_m - \varepsilon_d)} \right], \qquad (1)$$

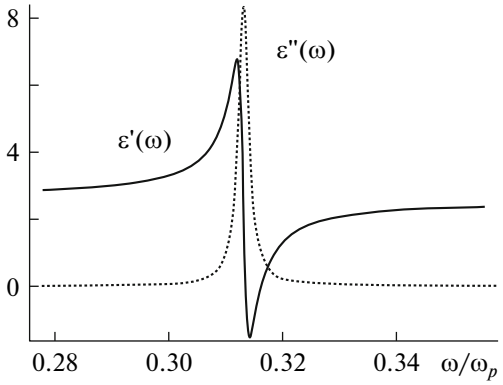

Fig. 1. Dependences of the imaginary $\varepsilon''_{mix}(\omega)$ (dashed line) and real $\varepsilon'_{mix}(\omega)$ (solid line) parts of effective permittivity ε_{mix} on normalized frequency ω/ω_p. The filling factor is $f = 0.01$.

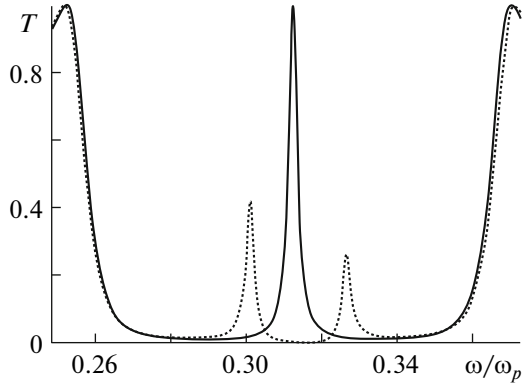

Fig. 2. Frequency dependence of transmission coefficient for the *s*-polarized waves at normal incidence of light upon the sample with the structural defect. The filling factor is $f = 0$ (solid line) and $f = 0.01$ (dashed line). The PhC comprises 19 layers: $(ab)^9 d(ba)^9$, $\varepsilon_a = 4.16$, $W_a = 50$ nm, $\varepsilon_b = 2.10$, $W_b = 74$ nm, and $W_d = 130$ nm. At $f = 0$ $\varepsilon_{mix} = \varepsilon_d = 2.56$. The light is incident onto the PhC from the medium with permittivity $\varepsilon_{ex} = 1$.

where f is the filling ratio, i.e., the fraction of nanoparticles in the matrix; ε_d and $\varepsilon_m(\omega)$ are the permittivities of the matrix and metal material, respectively; and ω is the optical frequency. The size of nanoparticles is much smaller than the wavelength and the field penetration depth. The permittivity of the metal from which nanoparticles are made can be found using the Drude approximation,

$$\varepsilon_m(\omega) = \varepsilon_0 - \frac{\omega_p^2}{\omega(\omega + i\gamma)}, \qquad (2)$$

where ε_0 is the constant that takes into consideration the contribution of interband transitions of bound electrons, ω_p is the plasma frequency, and γ is the inverse electron relaxation time.

The function $\varepsilon_{mix}(\omega)$ is complex,

$$\varepsilon_{mix}(\omega) = \varepsilon'_{mix}(\omega) + i\varepsilon''_{mix}(\omega). \qquad (3)$$

Neglecting the small factor γ^2, we can find the resonant frequency, which depends on the characteristics of the initial materials and the concentration of the dispersed phase f,

$$\omega_0 = \omega_p \sqrt{\frac{1-f}{3\varepsilon_d + (1-f)(\varepsilon_0 - \varepsilon_d)}}. \qquad (4)$$

At $\omega = \omega_0$, the function $\varepsilon'_{mix}(\omega)$ becomes zero, while $\varepsilon''_{mix}(\omega)$ acquires a greatest value. The function $\varepsilon'_{mix}(\omega)$ also vanishes at the point

$$\omega_1 = \omega_p \sqrt{\frac{1+2f}{(\varepsilon_0 + 2\varepsilon_d + 2f(\varepsilon_0 - \varepsilon_d))}}. \qquad (5)$$

Within the interval $[\omega_0, \omega_1]$ $\varepsilon'_{mix}(\omega) < 0$; i.e., the nanocomposite behaves like a metal in this frequency range.

The dielectric nanocomposite layer with a thickness of $W_d = 130$ nm consists of silver nanoballs that are suspended in a transparent optical glass. For silver, $\varepsilon_0 = 5.00$, $\omega_p = 9$ eV, and $\gamma = 0.02$ eV; for glass, $\varepsilon_d = 2.56$. Figure 1 shows the frequency dependences of the real and imaginary parts of the permittivity that were calculated using Eq. (1) for the filling factor $f = 0.01$.

As the volume concentration of nanoballs f increases, frequency ω_0 (4), corresponding to the resonance in the defect layer, shifts toward lower frequencies; under these conditions, the halfwidth of resonance curve $\varepsilon''_{mix}(\omega)$ changes insignificantly, while curve $\varepsilon'_{mix}(\omega)$ exhibits essential modifications, and the frequency range within which $\varepsilon'_{mix}(\omega) < 0$ widens.

RESULTS OF NUMERICAL ANALYSIS

As in [12], the transmission spectra for waves that propagate in the xz plane of a PhC with a nanodefect were studied using the transfer matrix technique [14]. As materials for alternating layers of the PhC, we considered zirconium dioxide (ZrO_2), the permittivity of which is $\varepsilon_a = 4.16$, and silicon dioxide (SiO_2), the permittivity of which is $\varepsilon_b = 2.10$. The thicknesses of the two layers were $W_a = 50$ nm and $W_b = 74$ nm, respectively. The light was incident onto the PhC from the outer medium with permittivity $\varepsilon_{ex} = 1$.

Figure 2 shows the transmission spectrum for the normal incidence of the light onto the PhC consisted of $N = 19$ layers (including the defect one). For filling factor $f = 0$, a seeding PhC with no dissipation is obtained. As is seen from Fig. 2, the seeding PhC is practically transparent for light with a frequency equal to that of defect mode ω_d located in the vicinity of center of the first bandgap. The bandgap lies in the wavelength range from 355 to 470 nm. The same figure

illustrates, for $f = 0.01$, the effect of splitting of the defect mode arising when resonant frequency of the nanocomposite ω_0 coincides with that of the defect mode ω_d. The value of the splitting is $\Delta\lambda \approx 34$ nm. The splitting of the defect mode frequency is observed at resonance when frequency of the nanocomposite ω_0 coincides with that of the defect mode ω_d. As quantity f increases from 0.01 to 0.1, the splitting increases by a factor of 3 up to 101 nm.

Figure 3 shows characteristic dependences of the transmission coefficients for *s*- and *p*-polarized waves for the case when $f = 0.01$. One can see from the figure that, for the *s*-polarized waves, splitting of the defect mode increases with increasing θ. In addition, an increase in the angle of incidence leads, in conformity with the Bragg condition, to a high-frequency shift of the bandgap boundaries. The frequencies of the two defect modes of the bandgap shift toward higher frequencies. This behavior of the frequencies can be understood by considering the defect mode of the PhC structure as a standing wave that arises due to reflections from the walls of the resonator formed by the nanodefect with thickness W_d. If, in addition, we neglect the frequency dependence of the refractive index in the region of the transmission peaks, then the resonance condition acquires the form $\lambda = 2W_d\sqrt{n^2 - \sin^2\theta}$, where n is the effective refractive index. Therefore, as angle of incidence θ increases, the modes shift toward higher frequencies, which is really observed in the numerical simulation. The transmission in the peaks of the defect modes with increasing detuning between the resonant frequency of the nanocomposite and that of the defect mode $\Delta\omega = \omega_d - \omega_0$ substantially changes and, at large angles, there remains only one high frequency peak in the bandgap corresponding to the initial defect mode. The transmission coefficients for the *s*- and *p*-type waves in the maximum of the high-frequency peak substantially differ at large angles of incidence. In particular, at $\theta = 40°$, the transmission in the maximum of the high-frequency peak for the *p*-waves is greater than that for the *s*-waves by a factor of 1.5. This is related to the fact that, in spite of the absence of the Brewster angle in the PhC structure under study, when the Fresnel reflection for the waves of the *p* type disappears at interfaces, one can observe an increase in the reflectivity for the *s*-polarized waves and a decrease in the reflectivity for the *p*-polarized waves with increasing angle of incidence (Fig. 3a).

The dependences of the splitting on the filling factor and the angle of incidence are presented in Fig. 4 for the *s*-polarized waves as compared with the waves of the *p*-polarization. As expected, at small angles of incidence, the splittings for the *s*- and *p*-type waves are almost the same. As θ increases, the splittings for the *s*- and *p*-polarized waves become different. A greater splitting of the defect mode for the *s*-polarized waves is

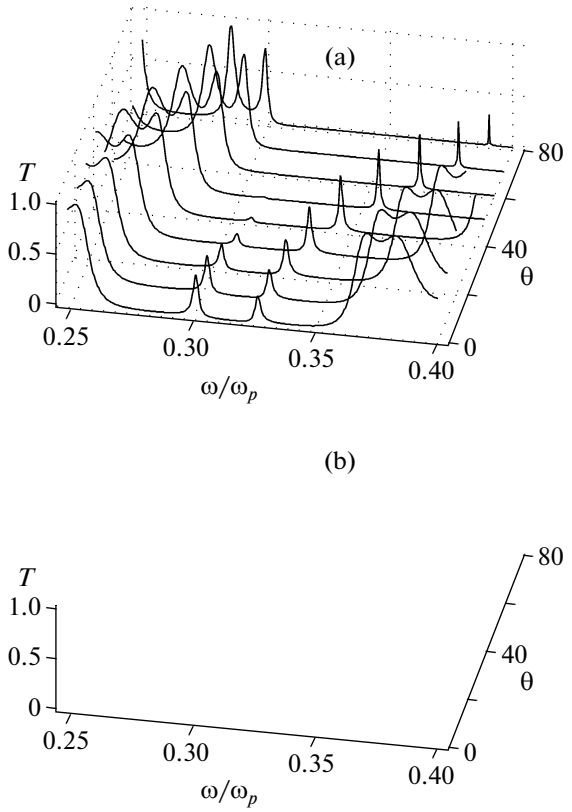

Fig. 3. Angular and frequency dependence of the PhC transmission coefficient for the *s* (a) and *p*- (b) polarized waves. The filling factor is $f = 0.01$.

likely to be related to the fact that, with increasing angle of incidence for *s*-waves, the bandgap broadens.

Brewster angle $\theta_B = \arctan(n_a/n_b)$ exists for the seeding PhC provided that the light is incident onto the PhC not from vacuum, but rather from the medium with permittivity $\varepsilon_{ex} = \varepsilon_b$. The transmission spectrum for the considered structure with $\theta_B = 54.6°$ is shown in Fig. 5a. One can see from the figure that, in the transmission spectrum, there arise additional bandgaps for the *s*- and *p*-polarized waves with practically coincident positions. The bandgap for the *s*-polarized waves arises in the continuous transmission spectrum and is related to the mixing of the resonant mode of the nanocomposite defect layer with photonic modes. For waves of the *p* type, which are polarized in the plane of incidence, a narrow bandgap is formed, with its width being determined by the frequency interval lying in the vicinity of resonance frequency ω_0 and corresponding to the maximum of $\varepsilon''_{mix}(\omega)$ (see Fig. 1). Outside this bandgap, the transmission coefficient is unity.

As an example, Fig. 5b shows the transmission spectrum for the *s*-polarized waves at an angle of incidence much smaller than the Brewster angle, when resonance frequency ω_0 appears to be close to the low-frequency boundary of the bandgap. The mixing of the

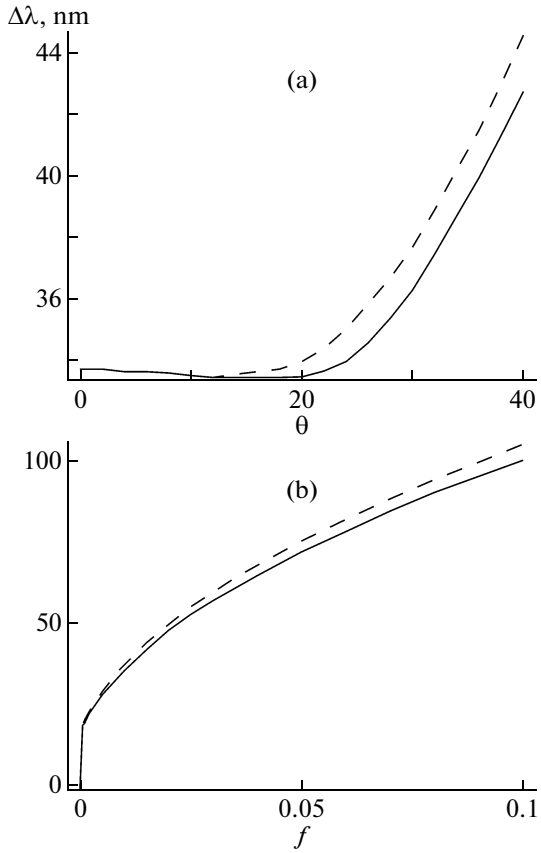

Fig. 4. Dependences of defect mode splitting Δλ on angle of incidence θ for filling factor $f = 0.01$ (a) and on filling factor f for the angle of incidence $\theta = 0$ (b); solid and dashed lines are for the p- and s-polarized waves, respectively.

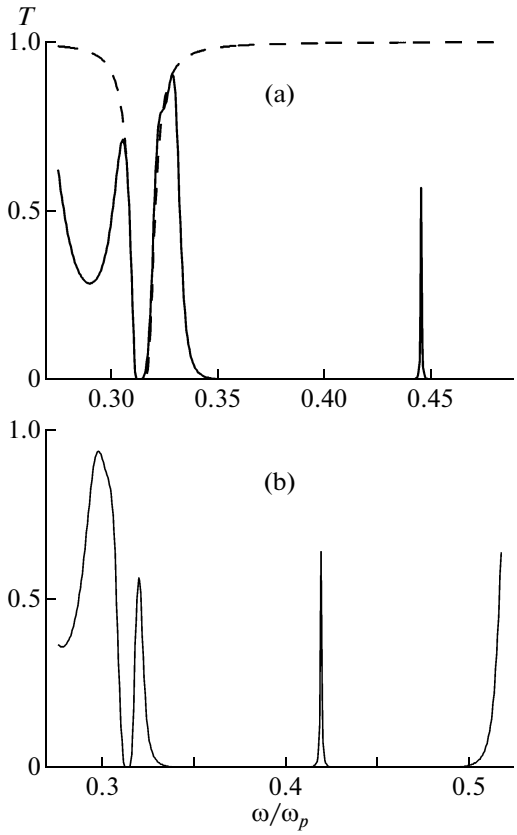

Fig. 5. Transmission spectrum of the PhC for different angles of incidence. (a) Brewster angle $\theta_B = 54.6°$, the solid and dashed lines are for the s- and p-polarized waves; (b) $\theta = 49.5°$. $f = 0.01$, s-polarization. The light is incident onto the PhC from the medium with permittivity $\varepsilon_{ex} = \varepsilon_b$.

resonant mode with photonic modes gives rise to the effect of splitting of the bandgap; i.e., there arises an additional transmission band in the bandgap, the width of which, 12.17 nm, is larger than the absorption bandwidth of the nanocomposite by 2.50 nm.

CONCLUSIONS

Transmission spectra of the s-polarized light waves of a one-dimensional photonic crystal with the resonant defect spectrum of a nanocomposite are studied. The revealed features of the spectra are mainly related to the resonant character of the effective permittivity of the nanocomposite and its essential dependence on the concentration of silver nanoballs in the dielectric matrix. It is shown that the splitting of the defect mode is highly sensitive to the concentration of nanoparticles and may attain 100 nm. It is established that, for specified filling factor f, the angular dependences of the transmission spectra for the s- and p-polarized waves substantially differ. It is shown also that, at an angle of incidence equal to the Brewster angle of the seeding PhC, an additional bandgap arises in the transmission spectrum for the s- and p-polarized waves. The occurrence of this band and its position are determined by the position of the resonant frequency in the transmission spectrum. The possibility of efficient controlling the PhC spectrum by varying the angle of incidence is shown. At a given value of filling factor f, there exist angles of incidence for which the transmission spectrum of the s-polarized waves of the PhC changes qualitatively and an additional transmission band arises.

Thus, we have demonstrated new possibilities of controlling the spectral and optical properties of 1D PhCs with resonant defect layers by varying the concentration of nanoballs and the angle of incidence.

ACKNOWLEDGMENTS

The work was supported by the grants NSh-7810.2010.3, RNP.2.1.1.3455, no. 27.1 and no. 3.9.1 RAS, no. 5 and no. 144 SO RAS, and g/k 02.740.11.0220 of the federal targeted program "Scientific and Pedagogical Personnel of Innovative Russia."

REFERENCES

1. A. M. Zheltikov, Usp. Fiz. Nauk **170**, 1203 (2000).
2. G. Liang, P. Han, and H. Wong, Opt. Lett. **29**, 192 (2004).
3. J. Vuckovic, M. Loncar, H. Mabuchi, and A. Scherer, Phys. Rev. E **65**, 016608 (2001).
4. O. Painter, R. K. Lee, A. Scherer, and A. Yariv, Science **284** (5421), 1819 (1999).
5. B. Shi, Z. M. Jeang, X. F. Zhon, and X. Wang, J. Appl. Phys. **91**, 6769 (2002).
6. T. V. Dolgova, A. I. Maidykovskii, M. G. Martem'yanov, et al., JETP Lett. **73**, 6 (2001).
7. T. M. Soljačić and J. D. Joannopoloulos, Nature Materials **3**, 211 (2004).
8. S. G. Tikhodeev and N. A. Gippius, Usp. Fiz. Nauk **179** (9), 1003 (2009).
9. P. N. D'yachenko and Yu. V. Miklyaev, Komp'yuternaya Optika **31** (1), 31 (2007).
10. A. N. Oraevskii and I. E. Protsenko, JETP Lett. **72**, 445 (2000).
11. J. C. Maxwell-Garnett, Philos. Trans. Roy. Soc. (London) **203**, 385 (1904).
12. S. Ya. Vetrov, A. Yu. Avdeeva, and I. V. Timofeev, JETP **113** (5), 755 (2011).
13. L. A. Golovan', V. Yu. Timoshenko, and P. K. Kashkarov, Usp. Fiz. Nauk **177** (6), 619 (2007).
14. P. Yeh, J. Opt. Soc. Am. **69**, 742 (1979).

Translated by V. Zapasskii